STOPBAND-EXTENDED BALANCED FILTERS USING BOTH λ/4 AND λ/2 SIRS WITH COMMON-MODE SUPPRESSION AND IMPROVED PASSBAND SELECTIVITY

S.-C. Lin[1, *] and C.-Y. Yeh[2]

[1]Faculty of Department of Electrical Engineering, National Chiayi University, Chiayi, Taiwan

[2]CSIE Department, National Chiayi University, Chiayi, Taiwan

Abstract—Benefitting from the simultaneous utilization of quarter-wave ($\lambda/4$) and half-wave ($\lambda/2$) microstrip resonators, a via-free balanced bandpass filter (BPF) with direct-coupled scheme is presented in this study. In the beginning, a single-ended filter with transmission zeros (TZs) is newly proposed and the mechanism of creating two TZs around the passband without necessitating cross couplings is adopted. The TZs can be made structure-inherent based on the coexisted out-of-phase couplings among a coupled-resonator pair. On the foundation of the presented single-ended filter, a balanced filter featuring extended differential-mode (DM) stopband, good common-mode (CM) suppression, and improved passband selectivity has been designed and implemented. The DM stopband extension is achieved by misaligning the higher-order harmonic frequencies of each resonator in the DM bisected circuit while the CM suppression is accomplished by both harmonic misalignment and careful designed coupled structure in the CM bisected circuit. Eventually, a demonstrated balanced filter centering at 1.5 GHz possesses DM stopband extended up to $8f_0^d$, where f_0^d denotes the DM operation frequency, and its CM rejection ratio (CMRR) within DM passband better than 51.9 dB is attained. For measurement convenience, the DM characterizations have been accomplished by 2-port network analyzer with simple rat-race baluns and are found relatively accurate within the -15 dB bandwidth of the utilized baluns.

1. INTRODUCTION

Balanced circuits have become the kernel of modern communication systems for years because of their many attractive characteristics. Basically, those balanced circuits designed with careful DM operation concepts [1] have good immunity from CM noises, cancellation of even-harmonic signals, elimination of via holes and etc.. Therefore, RF/Microwave components, such as antennas [2, 3], mixers [4–6], BPFs [7–15], and so on, are realized by their balanced counterparts. Among the conventional mobile devices, the SAW filters are usually employed in front-end modules with operation frequency not exceeding several gigahertzs (roughly around 3 GHz) because of their physical nature. However, new communication systems heading toward higher frequency are in rapid development thus SAW filters are no longer capable for serving as filtering components. For this reason, balanced filters play an indispensable role in the wireless communication systems. Those balanced filters based on coupled lines were presented in [7] and further improved in [8] with good common-mode suppression but with relatively high insertion loss. In addition, differential filter based on dual-mode resonators was constructed [9] by taking advantage of the double-sided parallel-strip line which is not favorable structure in integrated circuit design. Except CM suppression, both good stopband and selectivity are demanded in balanced BPFs. In [10], the adoption of proper SIRs for stopband extension and the introduction of cross couplings for creating the TZs ultimately restrict the balanced BPF layout. Through the utilization of bi-section quarter-wavelength ($\lambda/4$) stepped-impedance resonators (SIRs) and folded feed lines, the dual-band balanced BPF is achieved [11] but sacrifices the via-free property. Some balanced filters [12, 13] aim at dual-band applications but not at extended DM stopband. In [14, 15], Wu et al. adopted fully differential filters based on quasi-lumped resonators or transformers still without optimizing the out-of-band performance.

In this study, the design method for a novel direct-coupled balanced BPF based on coupled-resonator theory has been proposed by utilizing $\lambda/4$ and $\lambda/2$ SIRs. Our goal is to present a balanced filter with simple configuration, as well as high performances. The prototype of a single-ended bandpass filter possessing a pair of structure-inherent TZs is first proposed. Based on the single-ended filter, a balanced filter has then been designed and implemented by carefully considering its CM and DM perspectives. Benefitting from the higher-order resonance misalignment and careful investigation of DM and CM equivalent half circuits, the filter has extended stopband and good CM suppression. Furthermore, without introducing any cross couplings which may

perplex the filter configuration, two TZs contributed by special coupled structure can be observed around the filter passband for enhancing selectivity.

2. DESIGN CONCEPT OF BALANCED BPF

The schematic layout of the proposed 4th-order balanced filter is exhibited in Figure 1 with four standard single-ended ports 1, 1', 2, and 2' annotated. It is composed of two bi-section $\lambda/2$ SIRs and two full λ SIRs. To proceed smoothly, the two outer resonators are annotated as SIRs A and D while the two inner resonators are annotated as SIRs B and C. The resonant frequencies of utilized SIRs associated with two operation modes can be engineered in accordance with [16, 17]. The filter is symmetric with respect to the central dashed line. The Rogers RO4003c substrate ($\varepsilon_r = 3.55$, $h = 0.813$ mm, $\tan\delta = 0.0027$) is adopted in this study for implementing the proposed balanced filter. The simulated and measured mixed-mode S-parameters S^{mm} will be calculated from the simulated and measured standard 4-port S-parameters S^{std}.
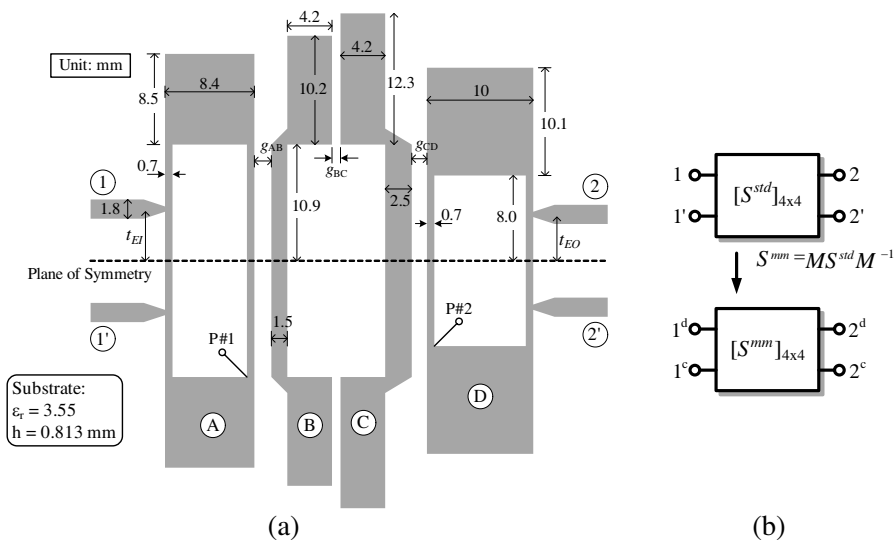

Figure 1. (a) Layout of the proposed balanced filter (Dimensions: $t_{EI} = 4.45$, $t_{EO} = 4.05$, $g_{AB} = 1.6$, $g_{BC} = 0.6$, and $g_{CD} = 1.42$ mm). (b) Transformation from standard S-parameters to mixed-mode ones [1].

Principally, the overall balanced filter design could be considered from the excitation viewpoints and concluded in three subsections as follows.

2.1. Single-ended Filter with Structure-inherent Transmission Zeros

Before introducing the design of filter under DM excitation, a single-ended filter is newly proposed as shown in Figure 3(a) to facilitate the discussion. The direct-coupled filter is designed with $f_0 = 1.5\,\text{GHz}$, $\Delta = 6.0\%$ for Butterworth response, where f_0 denotes filter center frequency and Δ indicates the fractional bandwidth (FBW). The utilized two resonator types are accordingly shown in Figure 2. In addition, all the $\lambda/2$ short-circuited SIRs (resonators 1 & 4) and $\lambda/4$ SIRs (resonators 2 & 3) are designed with same $R_z = 27.8\text{-}\Omega/56.2\text{-}\Omega$ and $u = 0.49$. The full-wave simulated results are shown in Figure 3(b). As can be seen, two TZs appear around the passband thus improve the selectivity without necessitating any cross couplings. Moreover,
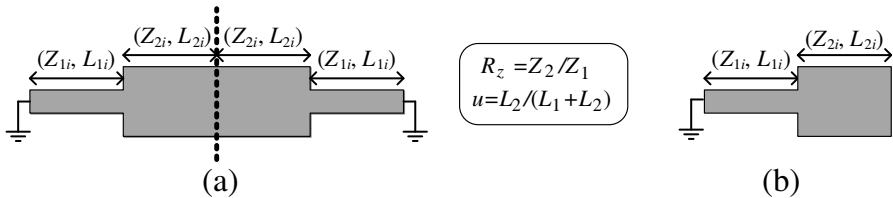

Figure 2. Adopted two types of resonators in the designate balanced filter under DM excitation. (a) $\lambda/2$ short-circuited SIRs ($i = A$ or D). (b) $\lambda/4$ SIRs ($i = B$ or C).
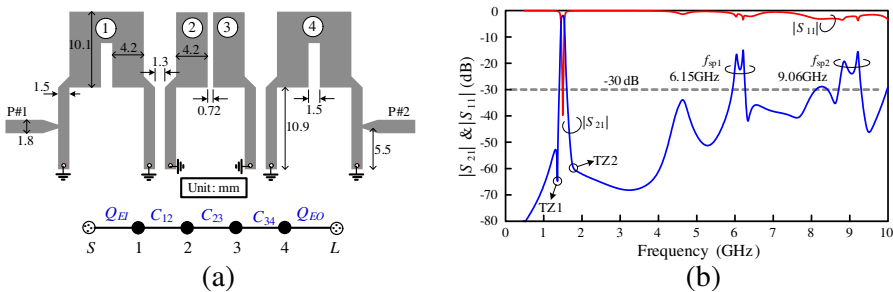

Figure 3. Newly proposed single-ended filter with structure-inherent TZs. (a) Filter layout. (b) Simulated results.
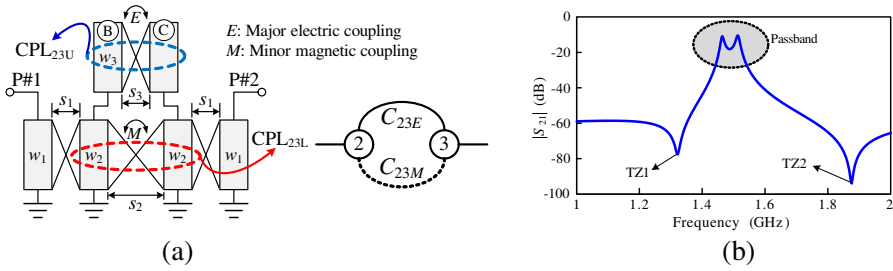
Figure 4. Structure for explaining the occurrence of two TZs around the passband due to out-of-phase couplings. (a) Coupled structure with dimensions in Figure 3 and coupling diagram. (b) Simulated transmission S_{21}.

two relatively significant spurious bands appear around 6.15 GHz (f_{sp1}) and 9.06 GHz (f_{sp2}), respectively. The two spurious bands f_{sp1} and f_{sp2} are caused by the simultaneous resonances of the four resonators. The coupled structure between resonators 2 and 3 is exhibited in Figure 4(a) while the corresponding full-wave simulated transmission coefficient is illustrated in Figure 4(b). The two TZs are contributed by the special arrangement of coupled structure between SIRs 2 and 3. The overall coupling coefficient C_{23} between SIRs 2 and 3 can be divided into electrical and magnetic couplings C_{23E} and C_{23M} produced by two pairs of coupled lines as annotated on Figure 4(a). Due to the simultaneous existence of the two components, the TZs will occur at the frequencies when the two out-of-phase couplings cancel as the similar but different implementation approach discussed in [18].

2.2. Migration from Single-ended Filter to Balanced One

Under differential-mode excitation, two resonator types, i.e., I/O short-circuited $\lambda/2$ SIRs and two inner $\lambda/4$ SIRs, which constitute the DM half-circuit filter as shown in Figures 2(a) and 2(b), respectively. Apparently, the DM bisected filter originates from the single-ended filter in Figure 3(a) with appropriate modifications. Assume the impedance ratio and length ratio defined as $R_{zi} = Z_{2i}/Z_{1i}$ and $u_i = L_{2i}/(L_{1i} + L_{2i})$ with $i = A$, B, C, and D. The design parameters R_{zi} and u_i for each resonator should be carefully selected to misalign the higher-order resonances of adjacent SIRs to achieve wide DM stopband. The balanced filter under DM excitation is designed with $f_0^d = 1.5$ GHz, $\Delta^d = 6.0\%$ for Butterworth response. With the given filter specification, the corresponding DM external quality factors and inter-stage coupling coefficients are: $Q_{EI}^{dd} = Q_{EO}^{dd} = 7.654$,
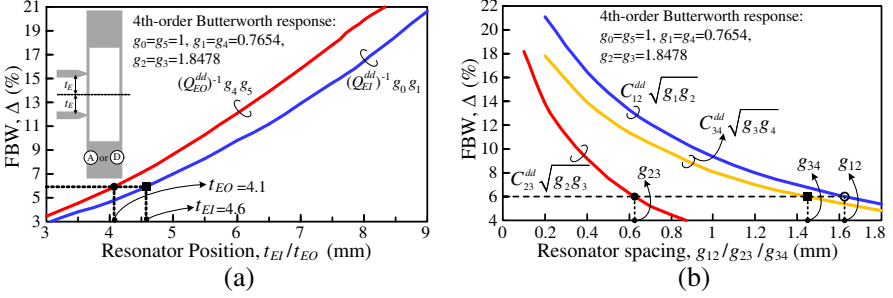
Figure 5. Adopted resonators in the designate balanced filter under DM excitation. (a) $\lambda/2$ short-circuited SIRs ($i = A$ or D). (b) $\lambda/4$ SIRs ($i = B$ or C).

$C_{AB}^{dd} = C_{CD}^{dd} = 0.084$ and $C_{BC}^{dd} = 0.054$. Among the filter, the couplings C_{AB}^{dd} and C_{CD}^{dd} are both realized by asymmetric shorted-end anti-parallel coupled lines while the coupling C_{BC}^{dd} is achieved by loaded open-end symmetric anti-parallel coupled line. The design charts of extracted quality factor and coupling coefficients for determining the physical dimensions of I/O tapped-line positions (t_{EI}/t_{EO}) and resonator spacings (g_{12}, g_{23}, and g_{34}) are displayed in Figures 5(a) and (b), respectively.

2.3. Common-mode Design

Alternatively, under CM excitation, two principal strategies are adopted for reducing the CM transmission. Firstly, since the design parameters of SIRs have been properly designed, the resonators in CM half-circuit also have the resonances misaligned/staggered (including fundamental one) and thus the transmissions are reduced at individual resonance of each SIR [19, 20]. It is worth mentioning that microwave signals transmit along the filter structure even the adjacent resonators do not resonate at the same frequency. Therefore, secondly, all the main couplings between adjacent resonators are now realized by edges of open-ended stubs in CM excitation which are physically lowpass structures to tackle the aforementioned issue. The simultaneous utilization of the two strategies ensures the reduction of transmitted CM signals to be optimized over wide frequency range.

3. FABRICATION AND MEASUREMENT OF BALANCED BPF

By adopting the DM and CM design concepts described in Section 2, a balanced filter (ckt-I) is then implemented. The impedance ratios are $R_{zA} = 0.19$, $R_{zB} = 0.49$, $R_{zC} = 0.68$, and $R_{zD} = 0.16\,\Omega/\Omega$ while the length ratios can be determined from Figure 1. To demonstrate the effect of the proposed techniques, another sample filter (ckt-II) resembling to the balanced filter configuration shown in Figure 1 but with all SIRs designed with $R_z = 27.8\text{-}\Omega/56.2\text{-}\Omega$ and $u = 0.49$ is additionally implemented for comparison. The simulation comparisons between the two filters are shown in Figure 6. As can be seen, the ckt-I filter possesses good behaviors from either DM or CM viewpoint. As for the ckt-II filter with DM bisected circuit identical to Figure 3(a), obvious spurious DM passbands arise around 6.15 and 9.15 GHz while spurious CM passbands occurs around 3.76 GHz. Therefore, as expected, the reduction of CM transmission and extension of DM stopband are significantly optimized in ckt-I because of the proposed techniques developed in Section 2. Although the adoption of dissimilar SIRs somehow destructs the filter symmetry along the vertical bisected line, the proposed balanced BPF has good DM stopband extension and CM suppression in return without increasing the complexity of resonator shapes. Since the adopted $\lambda/4$ and $\lambda/2$ SIRs possess relatively simple shapes, the optimization procedure would not take too much excess time according to our experience in comparison with that of those balanced BPFs utilizing resonators with complicated structures. For this reason, the resonance misalignment technique is still a good candidate for improving the filter performance.
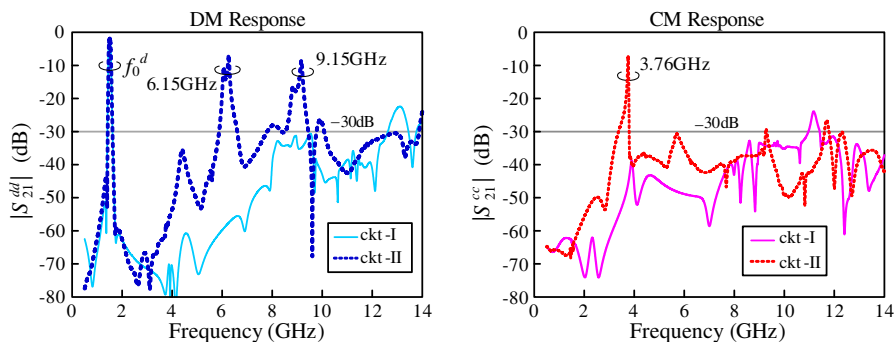

Figure 6. CM and DM simulation comparisons between ckt-I and ckt-II filters.

As a result, the photograph of the fabricated ckt-I filter in Figure 1 is displayed in Figure 7(a). The DM measured and simulated results of the filter are illustrated in Figures 7(b), (c), and (d). The measured DM center frequency f_0^d is at 1.508 GHz with the measured FBW 6.02% and minimum insertion loss of 2.48 dB. The DM stopband has been extended up to 12 GHz ($\approx 8 f_0^d$) with the rejection around 30 dB (except at 9.47 GHz with slightly lower rejection of 26 dB) and to 19.48 GHz with the rejection better than 25 dB. Moreover, two TZs occur at 1.38 and 1.79 GHz around the passband. To attain the equivalent circuit between SIRs B and C shown in Figure 4(a), the $\lambda/2$ SIRs are A and D hence adopted as I/O resonators. For the CM responses displayed in Figure 7(d), the CM signals are suppressed around the level of -60 dB near f_0^d. The CM stopband has been extended up to 13.73 GHz ($9.12 f_0^d$) with the satisfactory rejection of 30 dB. Figure 8 depicts the measured CM rejection ratio (CMRR = $|S_{21}^{dd}/S_{21}^{cc}|$) and the narrowband frequency response. The achieved CMRR is better than 51.9 dB among the 3 dB-passband and is superior to those of the published works [10]. The circuit size excluding feed lines occupies 39.8 mm $\times$ 46.4 mm ($0.199\lambda_0 \times 0.233\lambda_0$), where λ_0 is the free-space
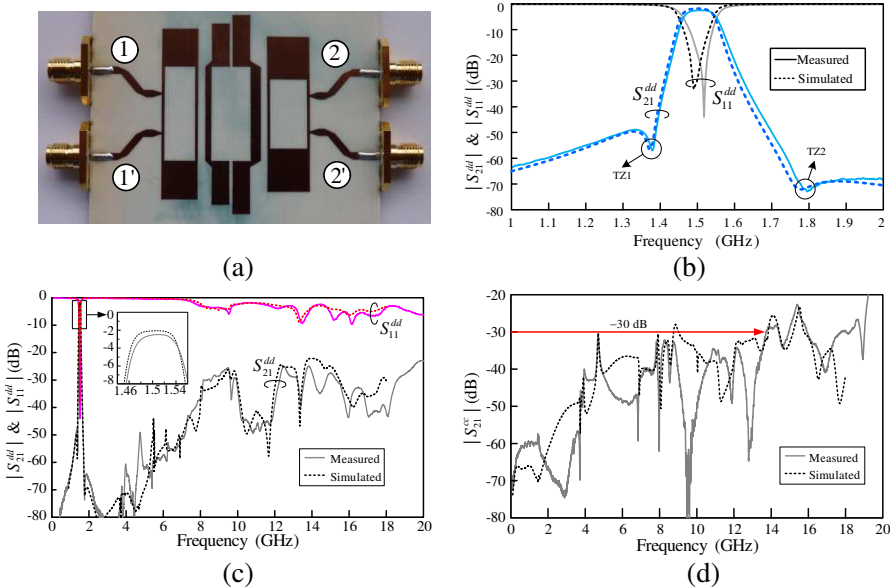

Figure 7. Proposed 4th-order balanced filter in Figure 1: (a) Circuit photograph. (b) Narrowband measured and simulated response. (c) Wideband DM response and (d) wideband CM response.
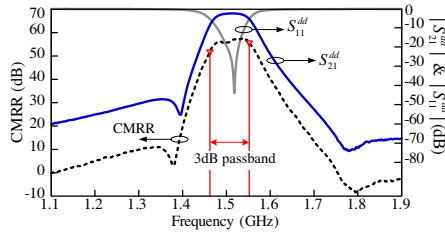
Figure 8. Measured CMRR and measured narrowband frequency response of the balanced filter in Figure 1.

guided wavelength at f_0^d. Note that the observable difference between CM measurement and simulation results from the fabrication mismatch due to chemical-etching imprecision. However, the DM response is less sensitive to this mismatch.

4. DM MEASUREMENT BY 2-PORT NETWORK ANALYZER

To directly and quickly characterizing the differential-mode performance by 2-port network analyzer (NWA), baluns are essential components in the measurement procedure [21]. Here, a transmission-line 3-port balun is realized based on the conventional 4-port rat-race hybrid by terminating the summation (Σ) port using $50\,\Omega$ load. Thus, if we inject signal from delta (Δ) port, the other two ports will provide equal-magnitude and out-of-phase output signals. On the other hand, once the signal enters from the DM port (i.e., ports 2 and 2'), the differential component will be in-phase combined in the SE port 1. Its corresponding mixed-mode S-parameters may be ideally expressed as

$$S_{Balun}^{mm} = \left[\begin{array}{cc} \begin{bmatrix} S_{11}^{ss} & S_{12}^{sd} \\ S_{21}^{ds} & S_{22}^{dd} \\ S_{21}^{cs} & S_{22}^{cd} \end{bmatrix} & \begin{bmatrix} S_{12}^{sc} \\ S_{22}^{dc} \\ S_{22}^{cc} \end{bmatrix} \end{array} \right] = \left[\begin{array}{cc} S_{Balun}^{dd} & S_{Balun}^{xm1} \\ S_{Balun}^{xm2} & S_{Balun}^{cc} \end{array} \right], \quad (1)$$

where S_{Balun}^{dd} and S_{Balun}^{cc} are the DM and CM S-parameters, respectively; S^{xm1} and S^{xm2} are the cross-mode S-parameters. As a result, S_{Balun}^{dd} features the DM characteristics of this 3-port network. Through network conversion [22], the chain matrix T_{Balun}^{dd} can be obtained.

The circuit photograph of the implemented TL balun is displayed in Figure 9(a) whiles the related measured mixed-mode S-parameters are shown in Figure 9(b). As can be seen, this balun maintains the cross-mode conversion (i.e., S_{21}^{cs}) below $-15\,\text{dB}$ from 1.142 to

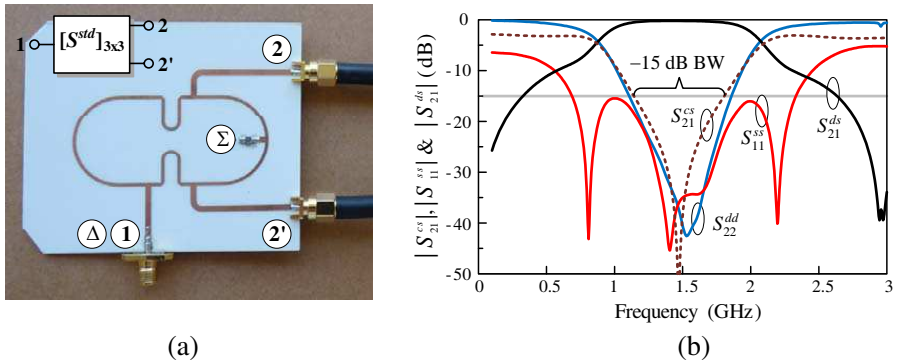(a)   (b)

Figure 9. Transmission-line (TL) balun based on the rat-race hybrid. (a) Photo of the fabricated circuit. (b) Measured mixed-mode scattering parameters with the -15 dB bandwidth indicated.
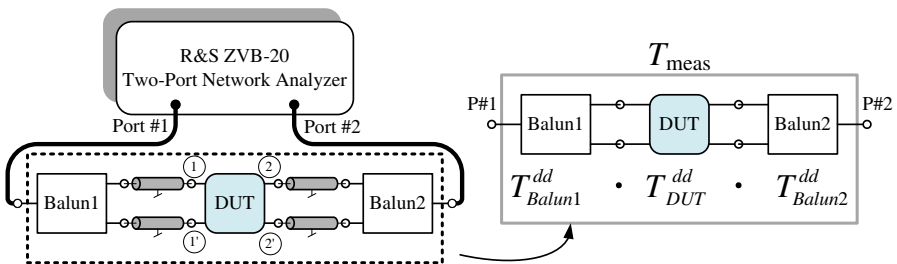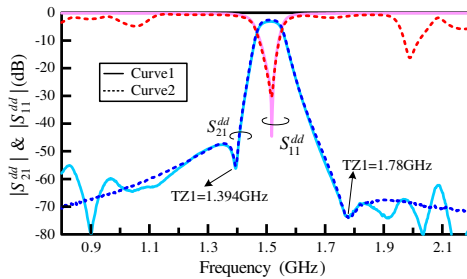

Figure 10. Instrument configuration for differential-mode measurement.

1.806 GHz. Moreover, in this range, the single-ended reflection coefficients S_{11}^{ss} at port 1 and the DM reflection coefficient S_{22}^{dd} at port 2 are also below -15 dB. In this study, we define the -15 dB bandwidth of balun for best DM characterization as the frequency range that all coefficients S_{21}^{cs}, S_{22}^{dd} and S_{11}^{ss} are measured below -15 dB.

With the realized baluns, one may configure the measurement as the arrangement shown in Figure 10(a). The required instrument and accessories are one 2-port VNA, two pairs of coaxial cables, and two identical baluns. Through two pairs of coaxial cable with precisely the same length and electrical property, the 1 and 1' ports of device under test (DUT) are connected to balanced ports of Balun 1 while the 2 and 2' ports of DUT are connected to balanced ports of Balun 2. After appropriate connection, Balun 1+DUT+Balun 2 can be considered as single component and measured by the 2-port VNA. The resultant 2-port S-matrix will be the DM S-parameters S^{dd} of the DUT. The main

Curve 1 (Solid line): Differential-mode measured results using the instrument configuration shown in Figure 10.

Curve 2 (Dashed line): Differential-mode results as shown in Figure 7(b) obtained from the transformation of measured standard 4-port S-parameters.

Figure 11. Measured DM S-parameters of the proposed balanced filter in Figure 1 based on the measurement configuration shown in Figure 10.

advantage of obtaining DM characterization based on 2-port VNA measurements is that the 4-port VNA much more expensive than 2-port one is not demanded. Theoretically speaking, the measurement range with good accuracy would coincide with the bandwidth of balun. Note that the measurement range can be further expanded by adopting baluns with wider bandwidth [23]. Another possible approach to get wideband measurement is dividing the frequency range into narrower bands and using the related baluns designed for different bands.

Due to the structure symmetry, the cross-mode conversions in baluns and filter under test may be almost neglected. Therefore, one may also evaluate the measurement results by multiplying the three DM chain ($ABCD$) matrices of the Balun 1, filter under test, and Balun 2 which may be transformed from their corresponding DM S-parameters. With this measurement setup, the acquired DM S-parameters of the proposed balanced filter in Figure 1 are illustrated as Curve 1 in Figure 11. Obviously, within the balun -15 dB bandwidth (i.e., 1.142 to 1.806 GHz), the measured results including S_{21}^{dd} and S_{11}^{dd} using the instrument configuration in Figure 10 coincide well with the mixed-mode results obtained from the transformation of measured standard 4-port S-parameters. It goes without saying that the S_{21}^{dd} of Curve 1 has insertion loss of 3.144 dB slightly higher than that of Curve 2 due to the usage of two additional baluns.

5. CONCLUSIONS

In this paper, a novel via-free balanced BPF comprises of both $\lambda/4$ and $\lambda/2$ SIRs is proposed. The filter is carefully designed from the DM and CM viewpoints for optimizing the filter performance. For the DM response, the filter possesses its DM stopband extended up to

$8f_0^d$ and two TZs are introduced around the passband by the delicate coupled structure containing coexisted out-of-phase couplings without requiring any cross couplings. Furthermore, the CM stopband has been skillfully extended up to $9.12f_0^d$. This balanced filter employs simple architecture to accomplish three good characteristics including extended stopband, excellent CM suppression and improved selectivity. In addition, the DM characterization has been carried out by 2-port NWA with simple TL balun based on ratrace hybrid. Within the -15 dB bandwidth of balun, the measured DM S-parameters coincide well with those acquired from transformation of measured standard 4-port S-parameters.

REFERENCES

1. Bockelman, D. E. and W. R. Eisenstant, "Combined differential and common-mode scattering parameters: Theory and simulation," *IEEE Trans. Microw. Theory Tech.*, Vol. 43, No. 7, 1530–1539, Jul. 1995.

2. Wang, F. J. and J. S. Zhang, "Wideband printed dipole antenna for multiple wireless services," *Journal of Electromagnetic Waves and Applications*, Vol. 21, No. 11, 1469–1477, 2007.

3. Kuo, F. Y. and H. T. Hsu, "Omni-directional dipole-based wideband planar antenna with capacitive end loading for WiMAX applications," *Journal of Electromagnetic Waves and Applications*, Vol. 24, No. 7, 959–969, 2010.

4. Guo, J., Z. Xu, C. Qian, and W.-B. Dou, "Design of a microstrip balanced mixer for satellite communication," *Progress In Electromagnetics Research*, Vol. 115, 289–301, 2011.

5. Lee, Y.-C., C.-M. Lin, S.-H. Hung, C.-C. Su, and Y.-H. Wang, "A broadband doubly balanced monolithic ring mixer with a compact intermediate frequency (IF) extraction," *Progress In Electromagnetics Research Letters*, Vol. 20, 175–184, 2011.

6. Lee, Y.-C., Y.-H. Chang, S.-H. Hung, W.-C. Chien, C.-C. Su, C.-C. Hung, C.-M. Lin, and Y.-H. Wang, "A single-balanced quadruple subharmonical mixer with a compact IF extraction," *Progress In Electromagnetics Research Letters*, Vol. 24, 159–167, 2011.

7. Lin, Y.-S. and C. H. Chen, "Novel balanced microstrip coupled-line bandpass filters," *Proc. URSI Int. Electromagn. Theory Symp.*, 567–569, 2004.

8. Wu, C.-H., C.-H. Wang, and C. H. Chen, "Novel balanced coupled-

line bandpass filters with common-mode noise suppression," *IEEE Trans. Microw. Theory Tech.*, Vol. 55, No. 2, 287–295, Feb. 2007.

9. Shi, J., J.-X. Chen, and Q. Xue, "A novel differential bandpass filter based on double-sided parallel-strip line dual-mode resonator," *Microw. Opt. Tech. Lett.*, Vol. 50, No. 7, 1733–1735, Jul. 2008.

10. Wu, C.-H., C.-H. Wang, and C. H. Chen, "Balanced coupled-resonator bandpass filters using multisection resonators for common-mode suppression and stopband extension," *IEEE Trans. Microw. Theory Tech.*, Vol. 55, No. 8, 1756–1756, Aug. 2007.

11. Lee, C.-H., I.-C. Wang, and C.-I. G. Hsu, "Dual-band balanced BPF using $\lambda/4$ stepped-impedance resonators and folded feed lines," *Journal of Electromagnetic Wave and Applications*, Vol. 23, Nos. 17–18, 2441–2449, 2009.

12. Hsu, C. I. G., C.-C. Hsu, C.-H. Lee, and H.-H. Chen, "Balanced dual-band BPF using only equal-electric-length SIRs for common-mode suppression," *Journal of Electromagnetic Waves and Applications*, Vol. 24, Nos. 5–6, 695–705, 2010.

13. Lee, C.-H., C.-I. G. Hsu, H.-H. Chen, and Y.-S. Lin, "Balanced single- and dual-band BPFs using ring resonators," *Progress In Electromagnetics Research*, Vol. 116, 333–346, 2010.

14. Wu, S.-M., C.-T. Kuo, P.-Y. Lyu, Y.-L. Shen, and C.-I. Chien, "Miniaturization design of full differential bandpass filter with coupled resonators using embedded passive device technology," *Progress In Electromagnetics Research*, Vol. 121, 365–379, 2011.

15. Wu, S.-M., C.-T. Kuo, and C.-H. Chen, "Very compact full differential bandpass filter with transformer integrated using integrated passive device technology," *Progress In Electromagnetics Research*, Vol. 113, 251–267, 2011.

16. Kuo, J.-T. and E. Shih, "Microstrip stepped impedance resonator bandpass filter with an extended optimal rejection bandwidth," *IEEE Trans. Microw. Theory Tech.*, Vol. 51, No. 5, 1554–1559, May 2003.

17. Yang, R.-Y., C.-Y. Hung, and J.-S. Lin, "Design and fabrication of a quad-band bandpass filter using multi-layered sir structure," *Progress In Electromagnetics Research*, Vol. 114, 457–468, 2011.

18. Lin, S.-C., C.-H. Wang, and C. H. Chen, "Novel patch-via-spiral resonators for the development of miniaturized bandpass filters with transmission zeros," *IEEE Trans. Microw. Theory Tech.*, Vol. 55, No. 1, 137–146, Jan. 2007.

19. Lin, S. C., P. H. Deng, Y. S. Lin, C. H. Wang, and C. H. Chen,

"Wide-stopband microstrip bandpass filters using dissimilar quarter-wavelength stepped-impedance resonators," *IEEE Trans. Microw. Theory Tech.*, Vol. 54, No. 3, 1011–1018, Mar. 2006.

20. Wu, H.-W., S.-K. Liu, M.-H. Weng, and C.-H. Hung, "Compact microstrip bandpass filter with multispurious suppression," *Progress In Electromagnetics Research*, Vol. 107, 21–30, 2010.

21. Bockelman, D. E. and W. R. Eisenstant, "Pure-mode network analyzer for on-wafer measurements of mixed-mode S-parameters of differential circuits," *IEEE Trans. Microw. Theory Tech.*, Vol. 45, No. 7, 1071–1077, Jul. 1997.

22. Pozar, D. M., *Microwave Engineering*, 3rd Edition, Wiley, New York, 2011.

23. Shao, W. and J.-L. Li, "A compact log-periodic branch-line balun with an octave bandwidth," *Journal of Electromagnetic Waves and Applications*, Vol. 25, Nos. 14–15, 2033–2042, 2011.